AJAE

Open Access

Vol. 16, No. 2, pp. 2021128, June 2022
doi: https://doi.org/10.5572/ajae.2021.128
ISSN (Online) 2287-1160, ISSN (Print) 1976-6912

Research Article

Experimental Characterization of $PM_{2.5}$ Organic Carbon by Using Carbon-fraction Profiles of Organic Materials

Shuichi Hasegawa[1),*]

[1)]Center for Environmental Science in Saitama, 914 Kamitanadare, Kazo, Saitama 347-0115, Japan

***Corresponding author.**
Tel: +81-480-73-8352
E-mail: hasegawa.shuichi@pref.saitama.lg.jp

Received: 19 October 2021
Revised: 2 March 2022
Accepted: 11 April 2022

ABSTRACT Organic aerosols (OA) in the atmosphere have complex emission sources and formation processes that must be determined to understand the OA composition and behavior. The thermal optical method is generally used to analyze organic carbon (OC) in OAs, and the resulting thermally fractionated OC profiles can be considered to be a synthesis of the organic materials contained in OAs. In this study, carbon-fraction profiles of 43 organic materials were determined and categorized into five types on the basis of their profile patterns. Then a chemical mass balance (CMB) analysis using the five types and the measured carbon-fraction profiles of particulate OC from various emission sources was conducted. The major sources thus determined were generally reasonable considering the known chemical properties of emission source particles. In addition, the seasonal organic matter composition in ambient particulate OC measured at a suburban site of Tokyo was experimentally estimated by a CMB analysis using the five types, and the potential of making good use of thermally fractionated OC data to understand the characteristics of OAs was discussed.

KEY WORDS Thermal optical method, Organic composition, Thermally fractionated organic carbon, Carbon-fraction profile, Emission source particle

1. INTRODUCTION

Most of the major chemical components of fine atmospheric particles typically have anthropogenic sources. Particles are derived from primary emissions such as combustion exhaust (e.g., elemental carbon; EC), or secondary production in the atmosphere such as sulfate and nitrate. Organic aerosol (OA) particles, however, are derived from both anthropogenic and natural sources, and they may originate as primary emissions or by secondary production. Therefore, their behavior in the atmosphere and their source contributions are complex. Because OAs consist of hundreds or even thousands of organic compounds (Hamilton *et al.*, 2004; Neusüss *et al.*, 2000; Turpin *et al.*, 2000), it is almost impossible to identify all organic materials in OAs. Instead, the organic carbon (OC) content, the total amount of carbon contained in OAs, is generally analyzed by the thermal optical method (Birch and Cary, 1996; Chow *et al.*, 1993), which determines concentrations of OC and EC fractions by stepwise heating in a helium or helium/oxygen

atmosphere with optical pyrolysis correction. The total OC concentration along with the concentrations of each OC fraction are then used to estimate the contributions of various OC sources by positive matrix factorization (PMF) (Murillo *et al.*, 2013, 2012; Chiou *et al.*, 2010; Cao *et al.*, 2006; Liu *et al.*, 2006; Kim and Hopke, 2004; Kim *et al.*, 2004). Although source particle profiles are not needed for PMF, to understand the PMF output, it is desirable to clarify the characteristics of the source carbon-fraction profiles.

The chemical mass balance (CMB) analysis determines quantitative relationships between source (emission source particles) and receptor (ambient particles), but the output depends on whether the given source profiles are appropriate for the measured receptor profiles. Basically, the model assumes that the chemical species are unchanged between source and receptor; thus, it targets primary particles rather than secondary particles. However, by including secondary species in source profiles, the contribution of secondary particles can also be estimated (Chen *et al.*, 2015; Lee *et al.*, 2008). The measured OC fractions of ambient particles represent a synthesis of the carbon-fraction profiles of organic materials in both primary and secondary particles. Therefore, if measured OC fractions of ambient particles could be reversely converted to organic matter compositions including secondarily produced materials, important information on formation processes and emission sources of OAs would be obtained.

In this study, the carbon-fraction profiles of 43 organic materials that are conceivable as primarily emitted or secondarily produced were determined, and then the profiles were categorized into five types by a cluster analysis. A CMB analysis was conducted using the five carbon-fraction profile types of organic materials as source profiles and OC measurements for not only primarily emitted but secondarily produced particles on various kinds of emission sources as receptor profiles, and the output was evaluated to determine its compatibility with the known chemical properties of primary and secondary particles. In addition, the organic matter composition of ambient particulate OC collected at a suburban Tokyo site was experimentally estimated by a CMB analysis using the five carbon-fraction profile types of the organic materials, and the results of the estimation were discussed.

2. DETERMINATION OF THE CARBON-FRACTION PROFILES OF ORGANIC MATERIALS

2.1 Methods

Carbon-fraction profiles of 43 organic materials, including *n*-alkanes, polycyclic aromatic hydrocarbons (PAHs), carboxylic acids, fatty acids, fatty alcohols, humic substances, sugars, sugar alcohols, and anhydro-sugars (Table 1), were determined by thermal optical analysis. *N*-alkanes, fatty acids, fatty alcohols, PAHs, and carboxylic acids are known as major components of primary and/or secondary OA and measured widely (Seinfeld and Pandis, 2006; Gelencsér, 2004). Humic substances, sugars, sugar alcohols, and anhydro-sugars are high-molecule materials and originated from natural matter, which are not so measured widely but were prepared for the variety of materials. The availability and solubility of the reagent were also considered. Solutions of the organic materials were prepared as follows: *n*-alkanes, fatty acids, and fatty alcohols were dissolved in hexane (500 ppm), PAHs were dissolved in acetonitrile (100 ppm), and humic substances were dissolved in aqueous sodium hydroxide (313 ppm for humic acid and 800 ppm for fulvic acid), whereas water was used as the solvent for carboxylic acids (1000 ppm), sugars and sugar alcohols (2000 ppm), and anhydro-sugars (800 ppm for levoglucosan and 2000 ppm for galactosan). All reagents used, except humic substances, were special grade. Humic substances obtained from ando and brown forest soils in Japan (Watanabe *et al.*, 1994) were supplied by the Japanese Humic Substances Society. The sample solutions (10 to 20 μL) were then applied to preheated quartz fiber filters (Pall, 2500QAT-UP, 8 mmφ) and analyzed by the IMPROVE analysis protocol by using a DRI model 2001A carbon analyzer (Chow *et al.*, 1993). Seven fractions were determined: OC1 (120°C), OC2 (250°C), OC3 (450 °C), and OC4 (550°C) in a He atmosphere, and EC1 (550°C), EC2 (700°C), and EC3 (800°C) in a 2% O_2 and 98% He atmosphere; however, the organic materials were not expected to include EC. The amount of pyrolyzed organic carbon (OCP) in each filter sample was also estimated by transmittance because of the sample solutions. Transmittance can sense the pyrolysis of the sample solution permeated into the whole cross section of the filter. Each sample was loaded into the analyzer as soon as the solvent had evaporated (eva-

Table 1. Organic materials used in this study and the type into which each was categorized on the basis of its carbon-fraction profile. Note that two kinds of humic substances, fulvic and humic acid, from two different soils (ando and brown forest soils) were used.

***n*-alkanes**		Type	**Fatty acids**		Type
Octadecane	C18	I	Palmitic acid	C16 : 0	III
Eicosane	C20	I	Stearic acid	C18 : 0	III
Tetracosane	C24	I	Oleic acid	C18 : 1	II
Pentacosane	C25	I	Lignoceric acid	C24 : 0	III
Hexacosane	C26	I	Melissic acid	C30 : 0	III
Triacontane	C30	II	**Fatty alcohols**		
Hentriacontane	C31	II	1-Octadecanol	C18	II
Tetracontane	C40	II	1-Tetracosanol	C24	II
Polycyclic aromatic hydrocarbons (PAHs)			1-Triacontanol	C30	–
Benzo[a]anthracene (BaA)		I	**Humic substances**		
Benzo[a]pyrene (BaP)		II	Fulvic acid		V
Benzo[b]fluoranthene (BbF)		II	Humic acid		III
Benzo[ghi]perylene (BghiP)		II	**Sugars**		
Benzo[k]fluoranthene (BkF)		II	Sucrose		II
Carboxylic acids			Galactose		II
Acetic acid	C2	III	Glucose		II
Oxalic acid	C2	IV	Fructose		II
Malonic acid	C3	III	Mannose		II
Succinic acid	C4	III	**Sugar alcohols**		
Maleic acid	C4 : 1	III	Mannitol		II
Glutaric acid	C5	III	Arabitol		II
Adipic acid	C6	III	**Anhydro-sugars**		
Azelaic acid	C9	III	Levoglucosan		II
Phthalic acid		III	Galactosan		I

poration time was no more than 30 min), and the organic solvents (hexane and acetonitrile) did not affect the analysis. The blank was as the same level as preheated filter (below 0.03 μgC) and the adsorption from ambient air was negligible. The analyzed carbon mass was 1.2 to 9.6 μgC except for sugars and sugar alcohols (9 to 20 μgC).

2.2 Results and Discussion

The carbon-fraction profile of each of the 43 organic materials was determined (Fig. 1). Note that the carbon-fraction profiles are analyzed by the IMPROVE protocol. The analyzed carbon amount in each organic material was generally consistent with the calculated amount. The general characteristics of the carbon-fraction profiles can be summarized as follows.

***n*-alkanes:** OC1 was the dominant fraction in compounds with relatively low carbon numbers such as eicosane (C20), and OC2 was the dominant fraction in those with high carbon numbers such as triacontane (C30), hentriacontane (C31), and tetracontane (C40). These results are consistent with the known greater volatility of *n*-alkanes with fewer carbons. The proportions of OC3, OC4, and OCP in *n*-alkanes were extremely low. One of the index which indicate the characteristics of *n*-alkanes is the carbon preference index (CPI), and the value of CPI is large when biogenic aerosols derived from higher plants are rich due to predominance of odd carbon number *n*-alkanes, whereas the value of CPI is close to 1 when the contribution of aerosols from fossil fuel burning become larger, which imply that *n*-alkanes show neither odd nor even carbon number dominance in aerosols from fossil fuel burning (Gelencser, 2004). However, the carbon-fraction profiles of adjacent odd and even carbon number *n*-alkane pairs, such as pentacosane (C25) and hexacosane (C26), and triacontane (C30) and hentriacontane (C31), were similar.

PAHs: OC1 was the dominant fraction in benzo[*a*]anthracene (BaA), which has four benzene rings, whereas OC2 was the dominant fraction in the other PAHs, which have five or more benzene rings. Thus, this result is consistent with the known greater volatility of PAHs with fewer benzene rings.

Carboxylic acids: OC4 was the largest fraction in oxalic

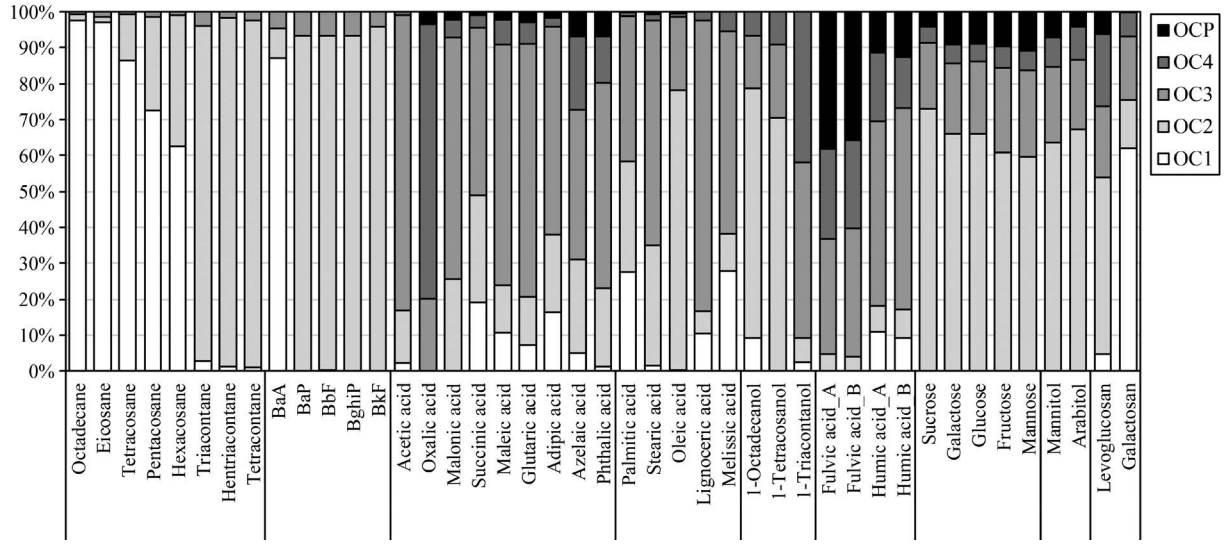

Fig. 1. Carbon-fraction profiles of the organic materials. Fulvic and humic acids A and B originated from ando and brown forest soils, respectively.

acid, which is generally the most abundant carboxylic acid in ambient aerosols (Kumagai, *et al.*, 2010; Kawamura and Yasui, 2005; Kawamura and Ikushima, 1993). In the other carboxylic acids, OC3 was the dominant fraction. Unlike the *n*-alkane and PAH profiles, the carbon-fraction profiles of the carboxylic acids did not show any trend related to carbon number. OCP was also found in the dicarboxylic acids, although in small proportions.

Fatty acids: OC1, OC2, and OC3 were the dominant fractions in the fatty acids, but the proportions of each differed. Palmitic acid (C16 : 0) and stearic acid (C18 : 0) are the main fatty acids found in ambient aerosols (Seinfeld and Pandis, 2006; Gelencsér, 2004). In palmitic acid, the proportions of OC1, OC2, and OC3 were similar, whereas in stearic acid, OC3 was dominant, and OC1 was hardly present. In contrast, the dominant fraction in oleic acid (C18 : 1), an unsaturated fatty acid, was OC2.

Fatty alcohols: The dominant fraction in 1-octadecanol (C18) and 1-tetracosanol (C24) was OC2, whereas both OC3 and OC4 were major fractions in 1-triacontanol (C30). Thus, unlike the fatty acids, fatty alcohols with higher carbon numbers had higher proportions of OC3 and OC4.

Humic substances: The carbon-fraction profiles of fulvic acid were dominated by OC3, OC4, and OCP, and the proportion of OCP was notably higher than that in the other organic materials. The carbon-fraction profiles of humic acid were similar to those of fulvic acid, except that in humic acid the proportion of OCP was lower and the proportion of OC3 was higher. In addition, the humic acid profiles, unlike the fulvic acid profiles, included OC1.

Sugars and sugar alcohols: The carbon-fraction profiles of sucrose, galactose, fructose, mannose, mannitol, and arabitol were very similar, and the OC2 fraction was dominant. OCP was also present in small proportions.

Anhydro-sugars: The levoglucosan profile was dominated by OC2, OC3, and OC4, whereas in galactosan, OC1 was the dominant fraction.

To examine the influence of carbon number, the carbon-fraction profiles of organic materials with the same number of carbons (C18, C24, or C30) among *n*-alkanes, fatty acids, and fatty alcohols were compared. Among C18 materials, OC1 was dominant in octadecane (*n*-alkane), OC2 was dominant in oleic acid (fatty acid) and 1-octadecanol (fatty alcohol), but OC3 was dominant in stearic acid (fatty acid). Among C30 materials, OC2 was dominant in the *n*-alkane (triacontane); OC3 was the dominant fraction, and the proportion of OC1 was relatively high in the fatty acid (melissic acid); and in the fatty alcohol (1-triacontanol), OC3 and OC4 were the dominant fractions. Among C24 materials, similar to C18 materials, OC1 was dominant in the *n*-alkane (tetracosane), and OC2 was dominant in the fatty alcohol (1-tetracosanol). However, the carbon-fraction pro-

file of the fatty acid (lignoceric acid) was similar to that of the C30 fatty acid (melissic acid), except with a larger proportion of OC3. Relationships among the profiles of *n*-alkanes, fatty acids, and fatty alcohols were not necessarily consistent, but the carbon-fraction profiles of fatty acids and fatty alcohols tended to include higher temperature fractions compared with those of the *n*-alkanes. In materials with fewer carbons (C18), the dominant fraction changed from OC1 in the *n*-alkane to OC2 and OC3 in the fatty acids and fatty alcohol, whereas in materials with more carbons (C30), the dominant fraction changed from OC2 in the *n*-alkane to OC3 and OC4 in the fatty acid and fatty alcohol.

In this study, a quartz fiber filter that the sample solutions were impregnated (followed by solvent evaporation) was used to determine the carbon-fraction profiles. The difference of the existing state of organic materials such as surface-to-volume ratio between impregnated solutions and airborne particles on a filter could affect the thermal behavior during the thermal optical analysis. A more realistic approach would be collecting particles on a filter produced by atomizing organic compound solutions. As for the sample analysis, the actual temperature at an analyzed filter sample is important to determine the carbon-fraction profiles. The difference between the setting temperature of IMPROVE protocol and the actual temperature at a filter sample is caused by the temperature control and the distance between a thermocouple and a filter sample. In the case of the DRI model 2001A carbon analyzer used in this study, the temperature control of OC1 (120°C) is not so fine compared to other fractions, though the difference was around 3 or 4°C in this study. With regards to the distance, the tip of the thermocouple is situated under the quartz boat that the filter sample is placed in the analyzer and thus the thermocouple is very close to the filter sample (around 2 or 3 mm). The variation of OC1 temperature affect to the reproductivity of OC1 fraction. Oher than that, the broad peak tailing of detector signal affect to the reproductivity of the OC fraction due to the procedure of dividing carbon-fraction by IMPROVE protocol. OC fractions are divided when the slope of the detector signal is closer to flat no matter whether the detector signal recover to the baseline or not, and thus the variation of dividing involve the following carbon fraction. Moreover, it is unavoidable that the relative standard deviation (RSD) of the minor carbon fraction (the fraction with low carbon mass) become larger (~150% in this study). However, the reproductivity of the minor carbon fraction less affect the carbon-fraction profile, because in this study the pattern similarity of the carbon-fraction profile is important (Section 3) and the major carbon fraction contributes to it much more than the minor carbon fraction. Several patterns of the carbon-fraction profile such as single fraction dominant (eicosane, tetracontane), double fraction dominant (hexacosane, oxalic acid, malonic acid, acetic acid, humic acid and sucrose), and triple fraction dominant (fulvic acid and levogulcosan) were examined, and the RSDs of the these major carbon fraction by 4 or 5 repetitions were relatively small such as OC1 of eicosane (1%), OC1 and OC2 of hexacosane (8% and 23%), OC3 and OC4 of oxalic acid (18% and 8%), OC3, OC4 and OCP of fulvic acid (7%, 12% and 23%). Among those fractions OC2 of hexacosane (23%) and OCP of fulvic acid (23%) were affected by the previous broad peak tailing. Note that the relatively worse RSD was found on levogulcosan (OC2 15%; OC3 23%; OC4, 25%).

3. CMB ANALYSIS OF THE CARBON-FRACTION PROFILES OF ORGANIC MATERIALS IN SOURCE PARTICULATE OC

3.1 Methods

For the CMB analysis, the carbon-fraction profiles of the 43 organic materials were first categorized into five types based on the results of a cluster analysis (Table 1). The cluster analysis was carried out by Ward's method using normalized data and squared distances. Type I comprised OC1-dominant organic materials, namely, C18–26 *n*-alkanes, the PAH with four benzene rings (BaA), and galactosan. Type II comprised the OC2-dominant organic materials, C30–40 *n*-alkanes, PAHs with five or more benzene rings, oleic acid (C18 : 1 fatty acid), C18 and C24 fatty alcohols, the sugars and sugar alcohols, and levoglucosan. Thus, *n*-alkanes and PAHs were categorized into Type I or II depending on the number of carbons or number of benzene rings, respectively. Type III comprised OC3-dominant organic materials, namely, the carboxylic acids (except for oxalic acid), the fatty acids (except for C18 : 1), and humic acid. Type IV contained only oxalic acid (dominantly OC4), and Type V contained only fulvic acid (which included OCP as a major fraction). Although 1-triacontanol was also

categorized individually, this was excluded from the CMB analysis, because the number of types must be five in order to solve the 5 by 5 matrix calculation in the CMB analysis and because 1-triacontanol is less abundant than either oxalic acid and fulvic acid in atmospheric aerosols.

Next, five carbon-fraction profile patterns were obtained by averaging the profiles of the organic materials in each type (Fig. 2); the standard deviations were used as the pattern uncertainties in the CMB analysis. Then, a CMB analysis using the five carbon-fraction profile patterns of the organic materials and particulate OC data from various kinds of emission sources was carried out. For this analysis, CMB 8.0 of the U.S. Environmental Protection Agency and an add-in software routine programmed in VBA for Microsoft Excel were used. Mathematical principle of the CMB model is simultaneous equations shown briefly as below.

$$C = \sum S_j \qquad j = \text{Type I, Type II, Type III, Type IV, Type V} \tag{1}$$

$$C_i = \sum A_{ij} S_j \qquad i = \text{OC1, OC2, OC3, OC4, OCP} \tag{2}$$

C represents measured concentration of OC, and C_i represents measured concentration of the *i*-th OC fraction. S_j is the contribution of the *j*-th type of carbon-fraction profile. A_{ij} is the fractional abundance of the *i*-th OC fraction in the *j*-th type of carbon-fraction profile. In this section C_i was normalized to unity because only the fraction profile needs to be obtained. The calculations were carried out by the effective variance least-squares method with elimination of negative contribution.

For the particulate OC data on emission sources, measurements of particulate emissions in the Tokyo metropolitan area (Tokyo Metropolitan Government, 2012a) were used in the CMB analysis. The emission sources, including fossil fuel combustion, biomass burning, cooking, and soil and road dust, are summarized in Table 2. Particles in the primary emissions were collected from flues by an Andersen stack sampler with a $PM_{2.5}$ cut-off. In addition, condensable particles were secondarily produced from gaseous materials by the air dilution method (dilution ratio 20) with a 16.7-L residence chamber (residence time 10 s at ambient temperature), and were collected on a quartz fiber filter. Sample air from flues was first passed through a $PM_{2.5}$ cyclone; thus, fine primary particles took a role as the condensation cores. The exhaust gas temperature was above 100°C (107 to 313°C) for natural gas, heavy oil, and incinerators, whereas below 100°C (56 to 81°C) for biomass and furnaces of steel and glass scraps (Tokyo Metropolitan Government, 2012b). The temperature at the gas meter of condensable particle sampling was around the ambient air temperature (8 to 44°C, depending on the season and the environment of the sampling place). Automobile exhaust emissions were sampled by using a chassis dynamometer, which collects primary particles only without size separation, and no condensable particle data were available for kitchen emissions. Further, only primary soil and road dust particles were collected by an air sampler in a small chamber by the resuspension method. The carbon-fraction profiles of emission source particles were determined by the thermal optical method in the same way as the organic materials (Section 2). The emission source particles were measured once for each emission source, and thus the measured data was given as it is, and a very small value (10^{-3}) was uniformly given as the standard deviation due to avoiding impossibility of calculation with no deviation. Note that it is very rare for chemical data on size-separated primary particles and secondarily produced condensable particles from various kinds of emission sources to be measured by the same method, even if the measurement for each emission source is only once.

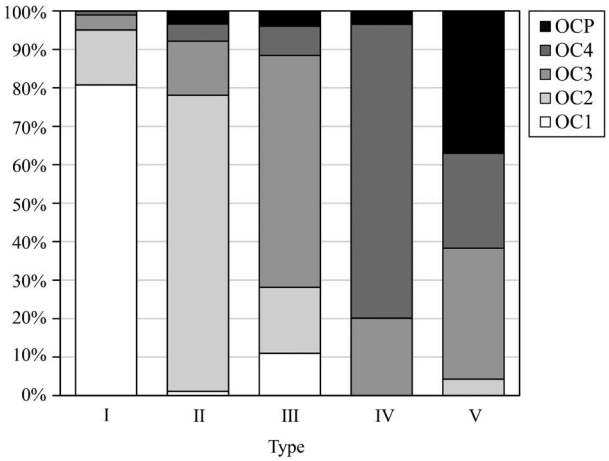

Fig. 2. The five patterns of carbon-fraction profiles determined by averaging the profiles of the organic materials in each type.

3.2 Results and Discussion

The results of the CMB analysis for particulate OC of the emission sources are shown in Fig. 3. The emission sources are roughly classified by fuel or burning material as following subsections.

Table 2. Emission sources used in this study (Tokyo Metropolitan Government, 2012a). An asterisk denotes particles not separated by size.

	Kinds of source	Emission source	Exhaust treatment
Fossil fuel combustion	Boiler A	Natural gas	Exhaust gas recirculation (EGR)
	Boiler B	Natural gas	None
	Engine	Natural gas	Diluted combustion
	Turbine	Natural gas	Denitration
	Boiler A	Heavy oil	None
	Boiler B	Heavy oil	Electrostatic precipitator and denitration
	Ship	Heavy oil	None
	Automobile A*	Light oil	EGR and oxidation catalyst
	Automobile B*	Light oil	EGR and urea catalyst
Waste incineration	Incinerator A	Municipal solid waste	Bag filter, scrubber, and denitration
	Incinerator B	Municipal solid waste	Bag filter, scrubber, and denitration
	Incinerator A	Sewage sludge	Ceramic filter and scrubber
	Incinerator B	Sewage sludge	Electrostatic precipitator and scrubber
Biomass burning	Biomass burning	Rice straw	None
	Biomass burning	Grass and pruned branches	None
	Boiler	Wood chips	Multicyclone
Cooking	Restaurant kitchen	Food	Grease filter
	Domestic kitchen	Food	None
Other	Furnace	Steel scrap	Bag filter
	Furnace	Glass scrap	Desulfurization and cyclone
	Soil dust	Soil dust particles	None
	Road dust	Road dust particles	None

3.2.1 Fossil Fuel Combustion

The results for primary and condensable particles in emissions from the two boilers, engine, and turbine fueled by natural gas were similar. Organic materials in Types II and III were the major components of primary particles, but organic materials in Type II were dominant in condensable particles, except those emitted by the turbine (dominantly Type I). The OC fraction profiles of the two boilers and the ship fueled by heavy oil were different. Type II was the major component of primary particles from boiler B and the ship, whereas Type V was dominant in those from boiler A. The χ^2 (the residual sum of squares) and r^2 (the coefficient of determination) in the CMB analysis results represent the fit of the model; the smaller χ^2 is, the better the result is, and the closer r^2 is to 1, the better the result is. χ^2 were ranged from 0.10 to 4.3 along with $r^2 \geqq 0.92$ except for the primary particles of boiler A, which was quite large (51) with $r^2 = 0.87$, and the carbon-fraction profile included a large EC1 fraction. By the pyrolysis correction, reflectance is used to divide the EC1 fraction into OCP and corrected EC1 amounts; thus, a large amount of EC1 in boiler A emissions may have led to overestimation of OCP through the influence of small reflectance variation. Type II was the dominant component in condensable particles from boiler A and the ship, whereas Type I was dominant in those from boiler B. This difference between boiler A and boiler B emissions might have been due to the exhaust treatment applied to boiler B (see Table 2); however, it is well known that fossil fuel combustion is the main emission source of alkanes and PAHs (categorized in Types I and II). The larger contribution of Type I to condensable rather than primary particles is reasonable, because alkanes with fewer carbons and PAHs with fewer carbon rings are more volatile.

The two automobiles (both with diesel-fueled engi-

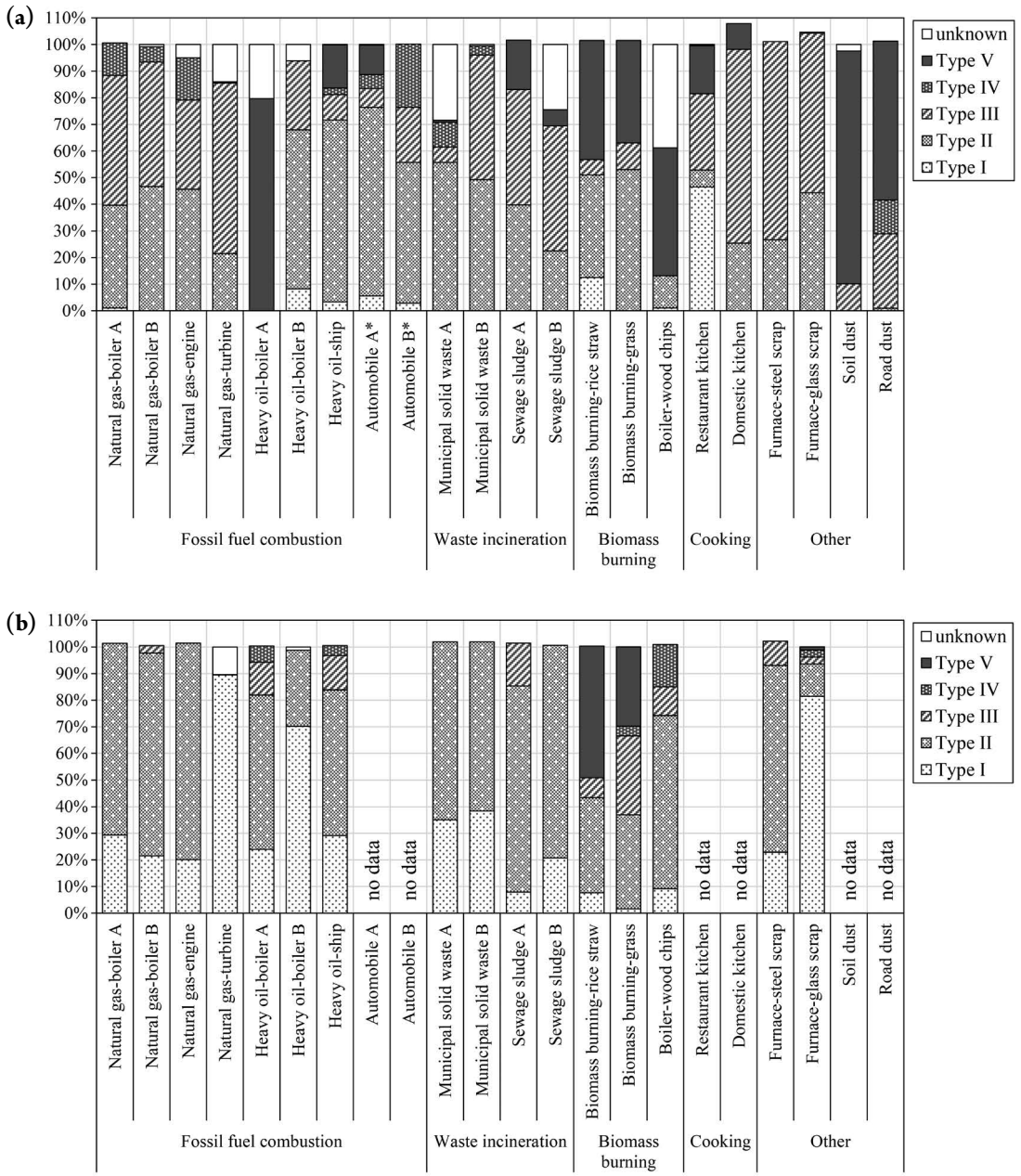

Fig. 3. Percentages of the five types of organic materials in particulate OC of the emission sources listed in Table 2 for (a) primary and (b) condensable particles, estimated by the CMB analysis. An asterisk denotes particles not separated by size.

nes) in general use at the time when the measurements were carried out (2008–2010) were in compliance with different emission regulations (those applied to new vehicles in 1997–1999 and 2005, respectively). However, Type II was the dominant component of emitted particles from both automobiles, although Types III and IV were also major components of particles from automobile B. χ^2 were 0.10 and 1.5 with $r^2 = 0.99$ and 0.98 for automobile A and B, respectively. PMF analyses have assigned diesel engine emission sources to carbon-fraction profiles dominated by OC2 or OC3 (Chiou *et al.*, 2010; Cao *et al.*, 2006; Liu *et al.*, 2006; Kim and Hopke, 2004; Kim *et al.*, 2004). These PMF results are consistent with the profiles obtained in this study because Type II is composed mainly of OC2, and Type III consists dominantly of OC3.

3.2.2 Waste Incineration

The fit of the model for waste incineration was calm ($\chi^2 = 0.42$ to 2.7, $r^2 \geqq 0.95$). The primary particle emissions from municipal solid waste incinerator A consisted mainly of Type II organic materials, and those of incinerator B were dominated by Types II and III. The condensable particle emissions of both incinerators were composed dominantly of Type II, followed by Type I. The difference in the primary particles might be due to differences in the waste composition. The primary particle results for incinerator B and the condensable particle results for both incinerators were similar to those for the boilers and engine fueled by natural gas.

The results for sewage sludge incinerators A and B were similar, although both Types II and III were major components of primary particles from sewage sludge incinerator A, whereas Type III was dominant in those from incinerator B. Condensable particles from both incinerators were mainly composed of Type II. The results for the two sewage sludge incinerators were roughly similar to those for municipal solid waste incinerator B.

3.2.3 Biomass Burning

The biomass burning results depended on whether rice straw, grass, or branches were burned. Type V was a major component of both primary and condensable particles, although Type II was a larger component than Type V of emissions from biomass burning of grass and branches. Type V was also a major component of primary particles emitted from the boiler fueled by wood chips, although χ^2 and r^2 were the worst (83 and 0.69, respectively). The carbon-fraction profile of the boiler fueled by wood chips included a large EC1 fraction, similar to boiler A fueled by heavy oil. Note that in the case of particles emitted from biomass burning of rice straw χ^2 and r^2 were slightly worse (4.1 and 0.89, respectively); however, except for the two cases χ^2 were ranged from 0.10 to 1.5 along with $r^2 \geqq 0.95$. Anhydro-sugars (e.g., levoglucosan) are used as tracers of biomass burning (Simoneit *et al.*, 1999), and total sugars are strongly correlated with levoglucosan (Scaramboni *et al.*, 2015). In addition, sugars such as mannose, glucose, and sucrose tend to correlate with levoglucosan (Theodosi *et al.*, 2018). The large contributions of Type II in the biomass burning results is consistent with these findings. Humic-like substances (HULIS) such as fulvic acid have been reported in atmospheric aerosols (Zheng *et al.*, 2013), and their emission sources include biomass burning (Salma *et al.*, 2010; Mayol-Bracero *et al.*, 2002), soil (Simoneit, 1980), plants (Salma *et al.*, 2010; Mukai and Ambe, 1986), and the ocean (Krivácsy *et al.*, 2008; Cavalli *et al.*, 2004). Notably, HULIS concentrations are higher in aerosols where biomass burning is being conducted (Lin *et al.*, 2010; Salma *et al.*, 2010; Mayol-Bracero *et al.*, 2002). Therefore, the high percentages of Type V in the biomass burning emissions in this study is consistent with these previous results. PMF analysis results have shown that OC3 is a major fraction in carbon-fraction profiles of wood smoke (Murillo *et al.*, 2013, 2012; Kim and Hopke, 2004; Kim *et al.*, 2004). This difference might be due to differences in the kinds of biomass being burned or the effects of meteorological parameters on open burning, or it might reflect model limitations.

3.2.4 Cooking

Cooking emission results differed between the domestic and restaurant kitchens. Type III was a larger component of the domestic kitchen emissions, whereas Type I was the dominant component of the restaurant kitchen emissions, followed by Type III. Oil content was also reported for lunch and dinner cooking in the domestic kitchen; thus, the emitted particles were likely to be rich fatty acids (Type III). Stearic, palmitic, and oleic acid are the main fatty acids in organic aerosols derived from cooking emissions (Zhao *et al.*, 2015). Although the reason for the different results between the domestic and restaurant kitchens is not obvious, they might reflect differences in the items cooked or in the exhaust treatment. Note the χ^2 were 2.4 and 0.14 with $r^2 = 0.94$ and 0.99 for the domestic and restaurant kitchens, respectively.

3.2.5 Other

The results for emissions from the furnaces that burned steel and glass scrap were similar. Types II and III were the major components of the primary particles. Type II was the major component of condensable particles from the furnace burning steel scrap, whereas Type I was the major component of the furnace burning glass scrap. Soil dust and road dust particles were mainly composed of Type V. Chow *et al.* (2003) have reported that OC3 and OC4 are the dominant OC fractions in dust from six different areas in California. Of course, because soil types can show large spatial differences, the dominant OC fractions of soils can differ between California and Tokyo. The predominance of Type V in the dust

particles in this study is not surprising because soils in Japan typically contain abundant HULIS. Note that χ^2 were ranged from 0.10 to 3.0 along with $r^2 \geqq 0.91$ for those four sources.

4. APPLICATION OF THE CMB MODEL TO AMBIENT PARTICULATE OC

4.1 Methods

Ambient $PM_{2.5}$ samples were collected with a low-volume air sampler (Thermo, FRM-2025) on preheated quartz fiber filters (Pall, 2500QAT-UP, 47 mmφ) during 24-h sampling periods. The sampling was carried out at Kazo, a suburban site 50 km from central Tokyo, from October 2013 to August 2014, and around 20 samples were collected during each season. A honeycomb activated carbon denuder (Thermo, 3500) was used to prevent positive sampling artifacts.

OC and EC in the samples were analyzed by the thermal optical method with a DRI model 2001A carbon analyzer (Chow *et al.*, 1993), and the IMPROVE analysis protocol was applied as described in section 2.1. The following seven fractions were estimated: OC1 (120°C), OC2 (250°C), OC3 (450°C), and OC4 (550°C) in a He atmosphere, EC1 (550°C), EC2 (700°C), and EC3 (800°C) in an atmosphere of 2% O_2 and 98% He. OCP was estimated from the reflectance of each filter sample.

The CMB analysis was carried out as described in section 3.1, using the averages and standard deviations calculated from the measurements obtained for each season.

4.2 Results and Discussion

The χ^2 and r^2 in the CMB analysis results were satisfactory ($\chi^2 \leqq 0.1$ and $r^2 \geqq 0.99$) for all seasons; thus, the fit of the model to the measurement data was good. In all seasons, Type V accounted for about 50% or more of all OC, followed by Type II (30–40%). The organic material of Type V was fulvic acid alone in this study, but only one study has reported fulvic acid concentrations in aerosols in Japan (Yamanokoshi *et al.*, 2014). According to Yamanokoshi *et al.* (2014), the average concentration of fulvic acid in aerosol particles with diameters smaller than 10 μm measured in Tokyo ranged from 0.6 μg/m^3 (summer) to 1.3 μg/m^3 (autumn) (from 0.3 to 0.6 μg/m^3 as OC). For comparison, the average OC concentration in $PM_{2.5}$ in Tokyo during the four seasons ranged from 2

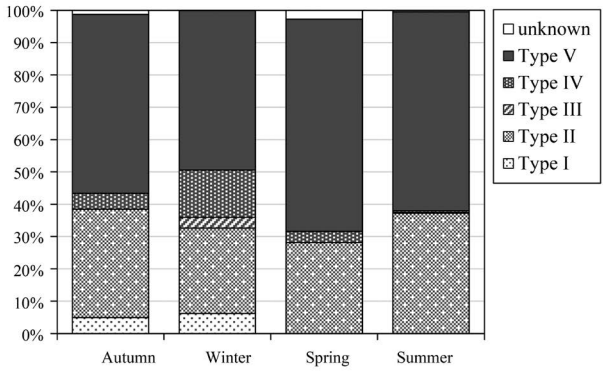

Fig. 4. Percentages of the five types of organic materials in ambient particulate OC measured in Kazo, estimated by the CMB analysis.

to 3 μg/m^3. Although the measured particle size fraction and the measurement period and site were not the same for fulvic acid and OC, these results indicate that fulvic acid accounts for roughly 20% of OC in aerosols in Tokyo. Therefore, the estimated contributions of Type V at Kazo in this study are different from the fulvic acid contributions reported by Yamanokoshi *et al.* (2014) for aerosols measured in Tokyo. Yamanokoshi *et al.* (2014) have suggested that HULIS in Tokyo are produced by secondary photochemical reactions in summer and by biomass burning in autumn. In summer, concentrations of photochemical oxidants are higher at Kazo than in Tokyo because Kazo is located downwind of Tokyo, whereas in autumn, biomass burning is conducted much more frequently around Kazo than in Tokyo. Therefore, the concentration of fulvic acid in aerosols may be higher at Kazo than in Tokyo. Type V was a major component of both primary and condensable particles from biomass burning (Section 3). However, the carbon-fraction profile of Type V includes a high proportion of OCP (Fig. 2), and other organic materials with a high proportion of OCP may not have been considered as Type V in this study. Therefore, the carbon-fraction profiles of more organic materials need to be investigated.

Type II is composed of organic materials that originated from fossil fuel combustion (*n*-alkanes and PAHs), biomass burning (levoglucosan and sugars), and biogenic emissions (sugars and sugar alcohols). Fossil fuel combustion emissions likely contributed to the aerosols collected during all four seasons, whereas biomass burning is conducted in a wide area around Kazo mainly in autumn. Biogenic emissions generally increase during the season

when vegetation is growing. Theodosi *et al.* (2018) have reported that mannitol concentrations, as well as glucose, fructose, and sucrose concentrations, increased throughout the growing season in aerosols sampled at a remote site in Crete. The seasonal differences in the Type II contribution may reflect increased biogenic emissions in summer (37%) and biomass burning emissions in autumn (34%). The percentage contributions of Type I, which were found only in autumn and winter, are reasonable, because the relatively more volatile materials of this type would form aerosol particles by condensation at low temperatures. Type III was found only in winter, and the highest Type IV contribution was also seen in winter. Type III consists of a mixture of various materials, mainly acids, and Type IV consists only of oxalic acid.

To verify the estimated organic matter composition, the comparison with the measured organic materials of the ambient samples is needed. The estimated organic matter composition is desired to be similar to seasonal trend of the measured organic materials that represent each type. However, considering that carboxylic acids are mostly produced photochemically, it would be difficult to explain the seasonal trends of Type III and IV. Also, the carbon-fraction profiles of more organic materials are needed to be analyzed in order to make better estimation of organic matter composition, especially because the only one compound was assigned to Type IV and V of the carbon-fraction profiles. In addition, as a limitation of this study, the carbon-fraction profiles are usable only for EC/OC measurements performed by IMPROVE protocol, since the database of emission source particles were compiled by IMPROVE protocol (Section 3), and ambient particles mostly analyzed by IMPROVE protocol in Japan. Different temperature protocols like a NIOSH (Peterson and Richards, 2002), EUSAAR2 (Cavalli *et al.*, 2010) or newly used IMPROVE_A (Chow *et al.*, 2007) have different temperature steps and so logically different carbon-fraction profiles. Nonetheless, this study would offer some clues of understanding the organic composition.

5. CONCLUSIONS

The carbon-fraction profiles of 43 organic materials among the *n*-alkanes, PAHs, carboxylic acids, fatty acids, fatty alcohols, humic substances, sugars, sugar alcohols, and anhydro-sugars were determined and categorized into five types. The major components of the carbon-fraction profiles of particulate OC from various emission sources, including fossil fuel combustion, waste incineration, biomass burning, and cooking, obtained by a CMB analysis using the five carbon-fraction profile types were generally reasonable considering the known chemical properties of emission source particles, though the large EC1 fraction of the emission source particles might make the fit of the CMB relatively worse. The seasonal compositions of ambient particulate OC measured at a suburban Tokyo site estimated by a CMB analysis using the five carbon-fraction profile types were partially consistent with expected seasonal differences. Although the type that OCP is the major fraction was found to be dominant in all seasons, the carbon-fraction profiles of more organic materials need to be investigated. The method presented in this study would offer some clues of understanding the organic composition from carbon-fraction profiles measured under the same conditions.

ACKNOWLEDGEMENT

This study was partially supported by Steel Foundation for Environmental Protection Technology, Japan (grant number 14atmos-217). Mr. S. Hayakari and Mr. R. Hanaishi provided the add-in software of CMB 8.0 of the U.S. E.P.A.

REFERENCES

Birch, M.E., Cary, R.A. (1996) Elemental carbon-based method for monitoring occupational exposures to particulate diesel exhaust. Aerosol Science and Technology, 25, 221–241. https://doi.org/10.1080/02786829608965393

Cao, J.J., Lee, S.C., Ho, K.F., Fung, K., Chow, J.C., Watson, J.G. (2006) Characterization of roadside fine particulate carbon and its eight fractions in Hong Kong. Aerosol and Air Quality Research, 6, 106–122. https://doi.org/10.4209/aaqr.2006.06.0001

Cavalli, F., Facchini, M.C., Decesari, S., Mircea, M., Emblico, L., Fuzzi, S., Ceburnis, D., Yoon, Y.J., O'Dowd, C.D., Putaud, J.P., Dell'Acqua, A. (2004) Advances in characterization of size-resolved organic matter in marine aerosol over the North Atlantic. Journal of Geophysical Research-Atmosphere, 109, D24215. https://doi.org/10.1029/2004JD005137

Cavalli, F., Viana, M., Yttri, K.E., Genberg, J., Putaud, J.-P. (2010) Toward a standardised thermal-optical protocol for

measuring atmospheric organic and elemental carbon: the EUSAAR protocol. Atmospheric Measurement Techniques, 3, 79–89. https://doi.org/10.5194/amt-3-79-2010

Chen, P., Wang, T., Hu, X., Xie, M. (2015) Chemical mass balance source apportionment of size-fractionated particulate matter in Nanjing, China. Aerosol and Air Quality Research, 15, 1855–1867. https://doi.org/10.4209/aaqr.2015.03.0172

Chiou, P., Shah, J., Lin, C.-J., Tadmor, R., Chu, H.-W., Ho, T.C. (2010) Source identification of Houston aerosol with carbon fractions in positive matrix factorization. International Journal of Environment and Development, 7, 135–152.

Chow, J.C., Watson, J.G., Pritchett, L.C., Pierson, W.R., Frazier, C.A., Purcell, R.G. (1993) The DRI thermal/optical reflectance carbon analysis system: description, evaluation and applications in U.S. air quality studies. Atmospheric Environment, 27A, 1185–1201. https://doi.org/10.1016/0960-1686(93)90245-T

Chow, J.C., Watson, J.G., Ashbaugh, L.L., Magliano, K.L. (2003) Similarities and differences in PM_{10} chemical source profiles for geological dust from the San Joaquin Valley, California. Atmospheric Environment, 37, 1317–1340. https://doi.org/10.1016/S1352-2310(02)01021-X

Chow, J.C., Watson, J.G., Chen, L.-W.A., Chang, M.C.O., Robinson, N.F., Trimble, D., Kohl, S. (2007) The IMPROVE_A temperature protocol for thermal/optical carbon analysis: maintaining consistency with a long-term database. Journal of the Air & Waste Management Association, 57, 1014–1023. https://doi.org/10.3155/1047-3289.57.9.1014

Gelencsér, A. (2004) Organic chemistry of aerosol. In Carbonaceous aerosol, Springer, New York, pp. 149–220.

Hamilton, J.F., Webb, P.J., Lewis, A.C., Hopkins, J.R., Smith, S., Davy, P. (2004) Partially oxidized organic components in urban aerosol using GCXGC-TOF/MS. Atmospheric Chemistry and Physics, 4, 1279–1290. https://doi.org/10.5194/acp-4-1279-2004

Kawamura, K., Ikushima, K. (1993) Seasonal changes in the distribution of dicarboxylic acids in the urban atmosphere. Environmental Science and Technology, 27, 2227–2235. https://doi.org/10.1021/es00047a033

Kawamura, K., Yasui, O. (2005) Diurnal changes in the distribution of dicarboxylic acids, ketocarboxylic acids and dicarbonyls in the urban Tokyo atmosphere. Atmospheric Environment, 39, 1945–1960. https://doi.org/10.1016/j.atmosenv.2004.12.014

Kim, E., Hopke, P.K. (2004) Improving source identification of fine particles in a rural northeastern U.S. area utilizing temperature-resolved carbon fractions. Journal of Geophysical Research, 109, D09204. https://doi.org/10.1029/2003JD004199

Kim, E., Hopke, P.K., Edgerton, E.S. (2004) Improving source identification of Atlanta aerosol using temperature resolved carbon fractions in positive matrix factorization. Atmospheric Environment, 38, 3349–3362. https://doi.org/10.1016/j.atmosenv.2004.03.012

Krivácsy, Z., Kiss, G., Ceburnis, D., Jennings, G., Maenhaut, W., Salma, I., Shooter, D. (2008) Study of water-soluble atmospheric humic matter in urban and marine environments. Atmospheric Research, 87, 1–12. https://doi.org/10.1016/j.atmosres.2007.04.005

Kumagai, K., Iijima, A., Shimoda, M., Saitoh, Y., Kozawa, K., Hagino, H., Sakamoto, K. (2010) Determination of dicarboxylic acids and levoglucosan in fine particles in the Kanto plain, Japan, for source apportionment of organic aerosols. Aerosol and Air Quality Research, 10, 282–291. https://doi.org/10.4209/aaqr.2009.11.0075

Lee, S., Liu, W., Wang, Y., Russell, A.G., Edgerton, E.S. (2008) Source apportionment of $PM_{2.5}$: Comparing PMF and CMB results for four ambient monitoring sites in the southeastern United States. Atmospheric Environment, 42, 4126–4137. https://doi.org/10.1016/j.atmosenv.2008.01.025

Lin, P., Huang, X.-F., He, L.-Y., Yu, J.Z. (2010) Abundance and size distribution of HULIS in ambient aerosols at a rural site in South China. Journal of Aerosol Science, 41, 74–87. https://doi.org/10.1016/j.jaerosci.2009.09.001

Liu, W., Wang, Y., Russell, A., Edgerton, E.S. (2006) Enhanced source identification of southeast aerosols using temperature-resolved carbon fractions and gas phase components. Atmospheric Environment, 40, S445–S466. https://doi.org/10.1016/j.atmosenv.2005.11.079

Mayol-Bracero, O.L., Guyon, P., Graham, B., Roberts, G., Andreae, M.O., Decesari, S., Facchini, M.C., Fuzzi, S., Artaxo, P. (2002) Water-soluble organic compounds in biomass burning aerosols over Amazonia 2. Apportionment of the chemical composition and importance of the polyacidic fraction. Journal of Geophysical Research, 107(D20), 8091. https://doi.org/10.1029/2001JD000522

Mukai, H., Ambe, Y. (1986) Characterization of a humic acid-like brown substance in airborne particulate matter and tentative identification of its origin. Atmospheric Environment, 20, 813–819. https://doi.org/10.1016/0004-6981(86)90265-9

Murillo, J.H., Ramos, A.C., García, F.Á., Jiménez, S.B., Cárdenas, B., Mizohata, A. (2012) Chemical composition of $PM_{2.5}$ particles in Salamanca, Guanajuato Mexico: Source apportionment with receptor models. Atmospheric Research, 107, 31–41. https://doi.org/10.1016/j.atmosres.2011.12.010

Murillo, J.H., Marin, J.F.R., Roman, S.R., Guerrero, V.H.B., Arias, D.S., Ramos, A.C., Gonzalez, B.C., Baumgardner, D.G. (2013) Temporal and spatial variations in organic and elemental carbon concentrations in PM_{10}/$PM_{2.5}$ in the metropolitan area of Costa Rica. Central America, Atmospheric Pollution Research, 4, 53–63. https://doi.org/10.5094/APR.2013.006

Neusüss, C., Pelzing, M., Plewka, A., Herrmann, H. (2000) A new analytical approach for size-resolved speciation of organic compounds in atmospheric aerosol particles: Methods and first results. Journal of Geophysical Research, 105, 4513–4527. https://doi.org/10.1029/1999JD901038

Peterson, M.R., Richards, M.H. (2002) Thermal-optical-transmittance analysis for organic, elemental, carbonate, total carbon, and OCX2 in $PM_{2.5}$ by the EPA/NIOSH method, Proceedings of Symposium on Air Quality Measurement Methods and Technology, 1–20, Air & Waste Management Asso-

ciation, Pittsburg, PA.
Salma, I., Mészáros, T., Maenhaut, W., Vass, E., Majer, Z. (2010) Chirality and the origin of atmospheric humic-like substances. Atmospheric Chemistry and Physics, 10, 1315–1327. https://doi.org/10.5194/acp-10-1315-2010
Scaramboni, C., Urban, R.C., Lima-Souza, M., Nogueira, R.F.P., Cardoso, A.A., Allen, A.G., Campos, M.L.A.M. (2015) Total sugars in atmospheric aerosols: An alternative tracer for biomass burning. Atmospheric Environment, 100, 185–192. https://doi.org/10.1016/j.atmosenv.2014.11.003
Seinfeld, J.H., Pandis, S.N. (2006) Organic atmospheric aerosols. In Atmospheric Chemistry and Physics from Air Pollution to Climate Change, John Wiley & Sons, New York, pp. 628–690.
Simoneit, B.R.T. (1980) Eolian particulates from oceanic and rural areas-their lipids fulvic and humic acids and residual carbon. Physics and Chemistry of the Earth, 12, 343–352. https://doi.org/10.1016/0079-1946(79)90117-4
Simoneit, B.R.T., Schauer, J.J., Nolte, C.G., Oros, D.R., Elias, V.O., Fraser, M.P., Rogge, W.F., Cass, G.R. (1999) Levoglucosan, a tracer for cellulose in biomass burning and atmospheric particles. Atmospheric Environment, 33, 173–182. https://doi.org/10.1016/S1352-2310(98)00145-9
Theodosi, C., Panagiotopoulos, C., Nouara, A., Zarmpas, P., Nicolaou, P., Violaki, K., Kanakidou, M., Sempéré, R., Mihalopoulos, N. (2018) Sugars in atmospheric aerosols over the Eastern Mediterranean. Progress in Oceanography, 163, 70–81. https://doi.org/10.1016/j.pocean.2017.09.001
Tokyo Metropolitan Government (2012a) Report on the investigation of emission source of fine particulate matter (in Japanese), https://www.kankyo.metro.tokyo.lg.jp/air/air_pollution/torikumi/pm25-report2011.files/02_hassei.pdf (last accessed on Jan. 31, 2022).
Tokyo Metropolitan Government (2012b) $PM_{2.5}$ emission source profile data (in Japanese), https://www.kankyo.metro.tokyo.lg.jp/air/air_pollution/torikumi/pm2_5/pm2_5.files/PM-purofairingu.xlsx (last accessed on Jan. 31, 2022).
Turpin, B.J., Saxena, P., Andrewset, E. (2000) Measuring and simulating particulate organics in the atmosphere: problems and prospects. Atmospheric Environment, 34, 2983–3013. https://doi.org/10.1016/S1352-2310(99)00501-4
Watanabe, A., Itoh, K., Arai, S., Kuwatsuka, S. (1994) Comparison of the composition of humic and fulvic acids prepared by the IHSS method and NAGOYA method. Soil Science and Plant Nutrition, 40, 601–608. https://doi.org/10.1080/00380768.1994.10414299
Yamanokoshi, E., Okochi, H., Ogata, H., Kobayashi, Y. (2014) Behavior and origin of water-soluble humic-like substances in particulate matter in central Tokyo. Journal of Japan Society for Atmospheric Environment, 49, 43–52. https://doi.org/10.11298/taiki.49.43 (in Japanese with English abstract, figures, and tables).
Zhao, X., Hu, Q., Wang, X., Ding, X., He, Q., Zhang, Z., Shen, R., Lü, S., Liu, T., Fu, X., Chen, L. (2015) Composition profiles of organic aerosols from Chinese residential cooking: case study in urban Guangzhou, south China. Journal of Atmospheric Chemistry, 72, 1–18. https://doi.org/10.1007/s10874-015-9298-0
Zheng, G., He, K., Duan, F., Cheng, Y., Ma, Y. (2013) Measurement of humic-like substances in aerosols: A review. Environmental Pollution, 181, 301–314. https://doi.org/10.1016/j.envpol.2013.05.055